

## **UCLA**

### **UCLA Previously Published Works**

#### **Title**

Experimental study of a string-based counterflow wet electrostatic precipitator for collection of fine and ultrafine particles

#### **Permalink**

<https://escholarship.org/uc/item/54q8z14w>

#### **Journal**

Journal of the Air & Waste Management Association, 71(7)

#### **ISSN**

1096-2247

#### **Authors**

Sadeghpour, Abolfazl  
Oroumiyeh, Farzan  
Zhu, Yifang  
[et al.](#)

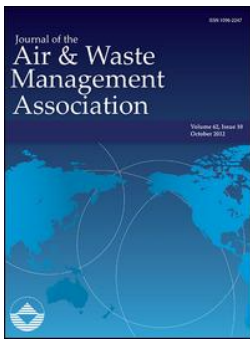
#### **Publication Date**

2021-07-03

#### **DOI**

10.1080/10962247.2020.1869627

Peer reviewed



## Experimental study of a string-based counterflow wet electrostatic precipitator for collection of fine and ultrafine particles

Abolfazl Sadeghpour , Farzan Oroumiyeh , Yifang Zhu , Danny D. Ko , Hangjie Ji , Andrea L. Bertozzi & Y. Sungtaek Ju

To cite this article: Abolfazl Sadeghpour , Farzan Oroumiyeh , Yifang Zhu , Danny D. Ko , Hangjie Ji , Andrea L. Bertozzi & Y. Sungtaek Ju (2021): Experimental study of a string-based counterflow wet electrostatic precipitator for collection of fine and ultrafine particles, Journal of the Air & Waste Management Association, DOI: [10.1080/10962247.2020.1869627](https://doi.org/10.1080/10962247.2020.1869627)

To link to this article: <https://doi.org/10.1080/10962247.2020.1869627>



Accepted author version posted online: 04 Jan 2021.



Submit your article to this journal [↗](#)



Article views: 81



View related articles [↗](#)



View Crossmark data [↗](#)

**Publisher:** Taylor & Francis & A&WMA

**Journal:** *Journal of the Air & Waste Management Association*

**DOI:** 10.1080/10962247.2020.1869627

## **Experimental study of a string-based counterflow wet electrostatic precipitator for collection of fine and ultrafine particles**

Abolfazl Sadeghpour<sup>a,\*</sup>, Farzan Oroumiyeh<sup>b</sup>, Yifang Zhu<sup>b</sup>, Danny D. Ko<sup>a</sup>, Hangjie Ji<sup>c</sup>, Andrea L. Bertozzi<sup>a,c</sup>, Y. Sungtaek Ju<sup>a</sup>

<sup>a</sup>Department of Mechanical and Aerospace Engineering, University of California Los Angeles, Los Angeles, CA, USA; <sup>b</sup>Department of Environmental Health Sciences, University of California Los Angeles, Los Angeles, CA, USA; <sup>c</sup>Department of Mathematics, University of California Los Angeles, Los Angeles, CA, USA; \*E-mail: abolfazlsad@ucla.edu.

### **Abstract**

Wet electrostatic precipitators (WESP) have been widely studied for collecting fine and ultrafine particles, such as diesel particulate matter (DPM), which have deleterious effects on human health. Here, we report an experimental and numerical simulation study on a novel string-based two-stage WESP. Our new design incorporates grounded vertically aligned polymer strings, along which thin films of water flow down. The water beads, generated by intrinsic flow instability, travel down the strings and collect charged particles in the counterflowing gas stream. We performed experiments using two different geometric configurations of WESP: rectangular and cylindrical. We examined the effects of the WESP electrode bias voltage, air stream velocity, and water flow rate on the number-based fractional collection efficiency for particles of diameters ranging from 10 nm to 2.5  $\mu\text{m}$ . The collection efficiency improves with increasing bias voltages or decreasing airflow rates. At liquid-to-gas (L/G) as low as approximately 0.0066, our design delivers a collection efficiency over 70% even for fine and ultrafine particles. The rectangular and cylindrical configurations exhibit similar collection efficiencies under nominally identical experimental conditions. We also compare the water-to-air mass flow rate ratio, air flow rate per unit collector volume, and collection efficiency of our string-based design with those of previously reported WESPs. The present work demonstrates a promising design for a highly efficient, compact, and scalable two-stage WESPs with minimal water consumption.

## **Keywords**

Wet Electrostatic Precipitator

String-based Direct Contact Mass Exchangers

Particulate Matter

## **Introduction**

Electrostatic precipitators (ESP) are widely used to collect particulate matters (PMs) from various exhaust streams. Important examples include exhausts from diesel engines and power plants, which represent some of the major particulate emitters in many developing countries.

Reducing the emission of particulate matters has attracted a lot of attention from researchers and governments due to its potential to cause severe health and environmental issues (Prasad and Bella 2011; Hesterberg et al. 2009; Lewtas 2007; Karanasiou et al. 2014; Pant et al. 2017; Pui, Chen, and Zuo 2014; Ristovski et al. 2012). In particular, current engine technologies and strict governmental regulations aim for reduction in particle emission rates of diesel engines (Fiebig et al. 2014). However, the benefit of emission rate reduction remains rather elusive.

Previous studies showed that the major portion of particles emitted from diesel engines are smaller than 2.5  $\mu\text{m}$  in aerodynamic diameter, commonly referred to as fine particles (Maricq 2006; Carotenuto, Di Natale, and Lancia 2010). Fine particles have greater impact on human health because they have elevated toxin burdens, can penetrate deep inside the respiratory system, and translocate into the circulation system (Pope et al. 2002; Yang et al. 2017; Dockery et al. 1993; Ning, Cheung, and Liu 2004; K.-H. Kim, Kabir, and Kabir 2015).

Among these fine particles, those with diameter less than 0.1  $\mu\text{m}$  are referred to as ultrafine particles and can be even more harmful to human respiratory and cardiovascular systems on a unit mass basis (HEI 2013; Ohlwein et al. 2019; Lane et al. 2016). Recently, these fine and ultrafine particles are also recognized to have malevolent effects on other parts of the human body such as the kidney (Xu et al. 2018).

Electrostatic precipitators utilize high-voltage electric fields and corona discharge to electrically charge particles, which are then collected on to plates of the opposite polarity. Traditional electrostatic precipitators can handle large volumes of gas (up to about 1900 m<sup>3</sup>/s), maintain a low pressure drop (less than 150 Pa), operate at high gas temperatures (up to 650°C), and deliver high overall mass collection efficiencies (Miller 2017).

However, traditional ESPs suffer from significant decrease in the collection efficiency for fine and ultrafine particles, with minimum typically occurring for particles of diameters around 0.2 to 0.5 µm (Mizuno 2000; Jaworek et al. 2018). This is within typical size ranges for many particulate emission sources, including diesel engines. Two-stage ESPs improves removal rates for fine particles by separating the charging and collection chambers. However, previous studies noted that, even with two-stage ESPs, the collection efficiency of fine particles remains low due to the re-entrainment effect inherent to traditional dry-type ESPs (Zukeran et al. 1999).

Wet electrostatic precipitators (WESP) help circumvent these issues by continuously running films of a liquid, typically water, to wash captured particles off the collector plates. WESP has been researched by many investigators, but many key challenges remain. These include high water consumption rates and corrosion of collector plates that cause dry spots and decrease the collection efficiency (Bayless et al. 2004). WESP are also ill-suited for direct particle capture from high-temperature exhausts because they quench the gas stream and lose collector water through evaporation.

To mitigate dry spots and corrosion of collectors, previous studies proposed new collector materials and designs, such as membrane-based collection plates, which utilize capillary force to maintain uniform films of water over the entire collection area (Hajrudin Pasic, Alam, and Bayless 2001; H. Pasic, Caine, and Shah 2006; C. Huang et al. 2014). Bayless and colleagues (Bayless et al. 2004) developed a parallel-plate, single-stage WESP using a membrane-based collection plate for collecting particles in the range of 1 to 25 µm. They observed that the collection efficiency on average was about 30% higher than that of dry ESPs with almost no attenuation in the collection efficiency for the smaller particles. Ali and colleagues (Ali et al. 2016) developed a single-stage cross-flow WESP design with vertical columns of membrane

cords supplied with water. They reported particle collection efficiencies greater than 80% for a particle size range of 1.61  $\mu\text{m}$  to 8.84  $\mu\text{m}$ . Neither studies, however, reported the collection efficiency for fine and ultrafine particles. Saiyasitpanich et al. (2006) experimentally examined a cylindrical single-stage WESP and reported high collection efficiencies for ultrafine particles (from 10 to 100 nm). However, the water-to-air flow rate ratio in their study was very high,  $\sim 0.9$  (kg-water/kg-air).

To help mitigate challenges of existing WESPs, we report a two-stage WESP design where liquid water beads traveling down along vertically aligned strings act as collection electrodes for a counterflowing exhaust gas stream. We performed a combined experimental and numerical simulation study to assess the performance of our design. Two different collection electrode configurations, rectangular and cylindrical, are implemented and examined in this work. The effects of the collector bias voltage, air velocity, and water flow rate per string on the collection performance were investigated experimentally. The particle trajectories and the effects of the water flow rate were studied using numerical simulation to help further understand the operation of our string-based collectors.

## Methods and Procedures

### Experimental setup

Figure 1 shows a schematic of the experimental setup used in this work to characterize the performance of our string-based two-stage WESPs. The experimental setup consists of four main sections: a diesel generator, a particle pre-charger, a particle collector (either rectangular or cylindrical configuration), and particle number concentration measurement systems.

A portable diesel engine (Sportsman GEN4000DF, 4 kW) served as the particle source in this study. An indirect air-cooled heat exchanger cooled down the generator exhaust from 200 ~ 350 °C down to less than 40 °C. The condensed water was collected in an in-line container. This cooling was necessary to protect the polymeric components in our prototype collectors and to mitigate significant evaporation of water from the collector strings. A flow diverter controlled the flow rate of the exhaust stream entering the charging cell. We varied the flow velocity in the charging region from 0.7 to 2 m/s, which corresponds to the flow velocity of 2 to 6 m/s in the collection region.

We examined two string based WESP configurations. The rectangular configuration consisted of five parallel strings of diameter 0.76 mm, which were placed 5 mm apart (Figure 2(a)). This configuration provides a 25 mm × 25 mm cross-sectional area for the air stream. The channel walls were made of a 3-mm-thick acrylic sheet. Two 0.5-mm-thick copper sheets placed on the outside of the air channel act as a high voltage electrode of the opposite polarity (see Figure 2(a)). The second configuration consisted of cylindrical cross section with a single vertical string at the center. The cylindrical configuration provided a circular cross-section of 25 mm in diameter for the air stream. Both WESP configurations were 0.6 m long.

A copper sheet covering the outside of the cylinder acted as a counter electrode and provided a symmetric electric field around the string. The copper sheet was placed outside of dielectric walls to prevent possible electric breakdown caused by water vapor. We note that high voltage electrode placed outside of the collector chamber wall can pose safety issues and that an

additional exterior insulation is necessary. The copper sheets were connected to a variable voltage source (0 - 10 kV) to investigate the effects of the collector voltage on the collection efficiency.

**Figure 1 here.**

Figure 1. Schematic of the experimental setup for characterizing the performance of the string-based collectors.

We used cotton fibers as strings in the present study. As shown in our previous works (Sadeghpour et al. 2019; Zeng, Sadeghpour, and Ju 2019), cotton threads absorb water and function as a super-hydrophilic surface. As a thin film of liquid flows down each string, intrinsic flow instability generates traveling water beads. These beads help wash collected particles efficiently and mitigate the re-entrainment issue. It also helps to eliminate potential dry spots at minimal water usage.

Water was supplied to the strings using stainless steel nozzles of 1.2 mm inner diameter connected to the top reservoir. The top water reservoir is grounded. A set of pumps and flow meters controlled the flow of water to the top reservoir. We varied the water flow rate per string in the range of 0.01 to 0.135 g/s by controlling the liquid height in the top reservoir to investigate its effects on the collection efficiency. The bottom reservoir with a weight-scale of 0.1 gram precision were used to measure the water flow rate.

A particle pre-charger (Figure 2(c) and (d)) is used to charge particles in the exhaust gas stream before being treated in WESP. The charging cell consists of three grounded parallel aluminum plates with thickness,  $t_{Al}$ , of 2 mm and length,  $L_p$ , of 10 mm. Two tungsten wires (200  $\mu\text{m}$  in diameter) were placed in between the plates. The plates are spaced 14 mm apart. Tungsten wires are connected to a high voltage source (0 - 20 kV). The applied voltage and the resulting corona current are measured using insulated digital multimeters. Since the cross-sectional area of the two WESP in this study are different, we designed two different pre-chargers with different heights. The height of the pre-charger,  $h_p$ , used for the cylindrical configuration is 60 mm and



that for the rectangular configuration is 80 mm. The other geometric parameters of the charging cells,  $L_p$  and  $w_p$ , are identical for both pre-chargers.

**Figure 2 here.**

Figure 2. Schematics of (a) the rectangular and (b) the cylindrical configuration on the left and (c) the particle pre-charger and the front view of the particle pre-charger used in this study on the right.

The particle size distributions were continuously monitored downstream of the collectors using two measurement systems: a SMPS (Scanning Mobility Particle Sizer; model 3080, TSI Inc., Shoreview, MN, USA) and a CPC (Condensation Particle Counter; model 3787, TSI Inc., Shoreview, MN, USA) for particles in the range of 10 nm to 300 nm and an APS (Aerodynamic Particle Sizer; model 3321, TSI Inc., Shoreview, MN, USA) for particles in the range of 0.5  $\mu\text{m}$  to 10  $\mu\text{m}$ . Table 1 summarizes the experimental conditions.

Table 1. Parameters and test conditions used to study the string-based WESP performance.

**Table 1 here.**

The performance of our two-stage WESPs, expressed in terms of the fractional particle collection efficiency,  $\eta$ , is given by the following expression:

$$\eta = \left(1 - \frac{C_{on}}{C_{off}}\right) \times 100 \quad (1)$$

where  $C_{on}$  and  $C_{off}$  are the number concentration of the particles (particles/cm<sup>3</sup>) the copper electrode in the collector was biased or not, respectively.

## Particle charging and collection model

Many previous studies investigated particle charging mechanisms and proposed various models (Lawless 1996; B. Y. H. Liu and Kapadia 1978; Benjamin Y. H. Liu and Yeh 1968). Predictions of these models agree reasonably well with the experimental results. We use the Cochet's charging model, which was shown to be valid for the particle size range of our main concern (from 0.1 to 1  $\mu\text{m}$ ) (Bai, Lu, and Chang 1995; Park and Chun 2002). This model predicts the maximum charge,  $Q_p$ , on particles as (Cochet 1961):

$$Q_p = \left[ \left( 1 + \frac{2\lambda}{d_p} \right)^2 - \left( \frac{2}{1 + \frac{2\lambda}{d_p}} \right) \left( \frac{\varepsilon_r - 1}{\varepsilon_r + 2} \right) \right] \pi \varepsilon_0 d_p^2 E_p \quad (2)$$

where  $\lambda$  is the mean free path of gas molecules,  $d_p$  is the diameter of the particles,  $\varepsilon_r$  is the dielectric constant of the particles,  $\varepsilon_0$  is the electrical permittivity of vacuum and  $E_p$  is the electrical field in the particle charging cell. Note that, DPMs are not chemically homogenous. In the present work, we treated  $\varepsilon_r$  as an adjustable parameter to compare the general trend of the collection efficiency as a function of the particle size.

Past studies also proposed various models for particle collection in ESPs (Riehle and Löfer 1995; Cooperman 1971; Zhibin and Guoquan 1994). Deutsch (Deutsch 1922) presented a simplified model by assuming perfect mixing which predicted the collection efficiency to be exponentially decreasing function of the length of the collection electrodes:

$$\eta = 1 - \exp\left(\frac{\varpi_m L}{\bar{U}_a S}\right) \quad (3)$$

where  $\varpi_m$  is the theoretical migration velocity of particles toward the collection plate due to the electric field (m/s),  $L$  is the length of the collection plate in the flow direction,  $\bar{U}_a$  is the mean velocity of the air stream, and  $S$  is the distance between the high-voltage electrode (copper sheets in this work) and the collection surface (strings). We obtain  $\varpi_m$  by balancing the Stokes' drag with the electrical force:

$$\bar{\omega}_m = \frac{Q_p E_c C_c}{3\pi\mu d_p} \quad (4)$$

where  $E_c$  is the pseudo-homogeneous electric field in the collector (V/m) and  $\mu$  is the gas dynamic viscosity.  $C_c$  is the Cunningham correction factor, which is given as follows (Flagan and Seinfeld 1988):

$$C_c = 1 + 1.246 \left(\frac{2\lambda}{d_p}\right) + 0.42 \left(\frac{2\lambda}{d_p}\right) \exp\left[-0.87 \left(\frac{d_p}{2\lambda}\right)\right] \quad (5)$$

### Numerical modeling

To help interpret our experimental results, we also performed a simplified numerical simulation study of electrohydrodynamic (EHD) using a commercial software package (COMSOL). The numerical simulation helps to visualize particle trajectories in our string based WESP and examine the particle charging and collection models presented in the previous section. Figure 3 shows the numerical simulation domains used in the present study: a 3D domain (Figure 3(a)) representing the rectangular WESP and a 2D axisymmetric domain (Figure 3(b)) representing the cylindrical WESP with a string of radius,  $R_s$ , 0.38 mm at the center.

### Figure 3 here.

Figure 3. Schematics of the numerical simulation domains for (a) the rectangular WESP and (b) the cylindrical WESP.

We solved the steady, incompressible, Navier-Stokes equations (Jewell-Larsen et al. 2008; Adamiak 2013) to first predict the velocity field of the air stream:

$$\nabla \cdot \vec{U}_a = 0 \quad (6)$$

$$\rho_a \vec{U}_a \cdot \nabla \vec{U}_a = -\nabla p + \mu_a \nabla^2 \vec{U}_a - \rho_a \nabla V \quad (7)$$

where  $\vec{U}_a$  is the velocity vector,  $p$  is the air pressure,  $V$  is the electric potential, and  $\rho_a$  and  $\mu_a$  are the density and dynamics viscosity of air, respectively.

To predict the trajectories of charged particles in the collector, we numerically solved the following equation, which considers the effect of drag force,  $\vec{F}_d$ , buoyancy force, and Coulomb's force,  $\vec{F}_e$ , (Q. Liu, Zhang, and Chen 2015):

$$m_p \frac{d\vec{U}_p}{dt} = \vec{F}_d + \frac{g(\rho_p - \rho_a)}{\rho_p} + \vec{F}_e \quad (8)$$

where  $m_p$  denotes the particle mass,  $g$  is the gravitational acceleration constant, and  $\rho_p$  is the particle density.

The drag force,  $\vec{F}_d$ , is calculated using (Kherbouche et al. 2016):

$$\vec{F}_d = \frac{1}{2} C_d S_p \rho_a |\vec{U}_p - \vec{U}_a| (\vec{U}_p - \vec{U}_a) \quad (9)$$

where  $\vec{U}_p$  is the velocity of particles,  $S_p$  is the cross-section of particles in the air flow ( $= \pi \cdot d_p^2 / 4$ ), and  $C_d$  is the drag coefficient for low Reynolds number (Parker 1997; Haider and Levenspiel 1989; Morsi and Alexander 1972), defined as follows:

$$C_d = \frac{24}{Re_p} \quad (10)$$

Here,  $Re_p$  is the particle Reynolds number defined using the particle diameter as the characteristic length. For air velocities considered in this study, equation 10 is a reasonable approximation for sizes as large as 1  $\mu\text{m}$ . Note that our primary focus was on sub-micron particles.

The electric force,  $\vec{F}_e$ , is obtained from:

$$\vec{F}_e = Q_p \vec{E}_c \quad (11)$$

$\vec{E}_c$ , the electric field vector in the collector, is in turn obtained from:

$$\vec{E}_c = -\nabla V \quad (12)$$

where  $V$  is the applied bias voltage to the collector string. In the simulations, it is assumed that the gas and particle distributions at the inlet are uniform. The initial values for the number of charges on the particles are assigned based on Eq. 2. A mesh-independence study was performed to ensure that the velocity and electric field distribution in the air stream and the number of collected particles do not change by more than 3% with further mesh refinement. The final computational meshes for the 2D domain (cylindrical collector) and the 3D domain (5-strings collector) contain approximately 80000 and 1950000 elements, respectively.

## Results and Discussion

Particle size distribution and electrical performance of the pre-charger

**Figure 4 here.**

Figure 4(a) shows the current-voltage relationship of the wire-plate particle pre-charger. The corona onset voltage (COV) in our particle pre-charger is 5.5 kV.**Figure 4 here.**

Figure 4(b) shows average over four independently measured particle size distributions at the inlet of the charging cell using SMSP and APS. Each SMPS data in turn consist of 10 consecutive size distribution measurements and each APS data include approximately 200 consecutive measurements. Size distributions obtained using SMPS and APS are merged using the TSI Data Merge Software Module (TSI Inc., Shoreview, MN). This software module converts electronic mobility diameters measured by SMPS to aerodynamic diameters and merge them with APS data. The composite size distributions are derived from fitting the merged data into a two- or three-mode distributions.

The particle precipitation rate of the pre-charger was less than approximately 15%. This was measured at the outlet of the overall set up in which the bias voltage and water flow rate at the collector strings were set to zero.

**Figure 4 here.**

Figure 4. (a) Voltage-current curve and (b) average particle size distribution at the inlet of the particle pre-charger.

Effects of water flow rate

Figure 5 shows the fractional collection efficiency of the two-stage cylindrical WESP as a function of the particle diameter. The water flow rates per string,  $\dot{m}_{LPS}$ , were fixed at 0.01, 0.08, or 0.135 g/s. The air velocities in the particle pre-charger and the collection zone were maintained at 1 and 3 m/s, respectively. The particle pre-charger and the string collector bias voltage were 7.4 kV and 10 kV, respectively. Under the bias voltage applied to the collector strings and the distance between the string collector and electrode, we did not observe any water jet or droplet emission from the string collectors. The results indicate that increasing the water flow rate per string has negligible effects on the collection efficiency. As discussed in our previous work (Sadeghpour et al. 2019), as the water flow rate increases, the number of water beads per string length increases. However, increasing the bead density has a negligible effect on the gas stream velocity profile and the electrical field in the particle collector partly because water beads only occupy less than 3% of the cross section in the collector (see Numerical simulation results for further discussion). As a result, increasing the water flow rate has a small effect on the particle collection efficiency.

**Figure 5 here.**

Figure 5. Effect of the water flow rate per string on the fractional collection efficiency of the cylindrical WESP.

As mentioned before, a water consumption rate necessary for cleaning the collection plates is an important consideration in WESP. Therefore, we use the liquid-to-gas mass flow rate ratio [kg-water/kg-air] as the key performance metric. Figure 6 shows the fractional collection efficiency of our design compared with that of other WESP designs as a function of the water-to-air mass flow rate ratio. Our string-based collector offers comparable collection efficiencies over a wide range of particle diameters at approximately one third of the water-to-air mass flow rate ratios.

**Figure 6 here.**

Figure 6. Collection efficiencies as a function of the liquid-to-gas flow rate ratio for different WESP devices. We compare our device with previously reported WESP devices; electrostatic droplet spray (Pilat 1975), cylindrical WESP for DPM (Saiyakitpanich et al. 2006), flat-plate WESP (H.-J. Kim et al. 2011), electrospray tower scrubber (H.-G. Kim et al. 2014), cross flow string-based WESP (Ali et al. 2016), wire-to-plate WESP (Yang et al. 2017), and self-flushing WESP (Su et al. 2018).

Previous studies reported high collection efficiencies (>95%) with different WESP designs when the air flow velocity in the collection chamber is very low (<0.2 m/s) (Teng, Fan, and Li 2020; Chen et al. 2014; W. Kim et al. 2015). To account for the effect of the air flow rate normalized with respect to the device size, we compare the air flow rate per unit collector volume as another useful metric in Table 2. This table also shows the air flow rate per unit collector volume of previously reported WESPs together with the corresponding experimental conditions, particle diameter ranges, and collection efficiencies. This comparison shows that the present string-based collector can achieve over 70% collection efficiencies at higher air flow rates per unit volume of the collector and at lower water consumption rates.

Table 2. Comparison of the experimental conditions and performance metrics of the present design with those of previous WESP designs.

**Table 2 here.**

## Effects of collector bias voltage

Figure 7 shows the fractional collection efficiency as a function of the particle size for the cylindrical and the rectangular WESP under different collector bias voltages. String collector bias voltage of 5 kV and 10 kV were tested. The applied bias voltages were not high enough to cause visible water jet or droplet emission from the string collectors. Also shown is the collection efficiency predicted using equations 2-5. A 7.2 kV bias voltage was used in the particle pre-charger, and the water flow rate per string,  $\dot{m}_{LPS}$ , was 0.06 g/s.

Increasing the collector bias voltage increases the particle collection efficiency for all particles larger than approximately 30 nm in diameter. However, for particles smaller than approximately 30 nm in diameter, the applied collector voltage has a negligible effect on the collection efficiency. This behavior, which was also reported in earlier studies (Yoo, Lee, and Oh 1997; Li and Christofides 2006; H.-J. Kim et al. 2011), is due to the fractional charging effect. Ultrafine particles have average acquired elementary charges of less than one. This implies that some of these particles do not acquire any electric charge in the pre-charger and are not collected efficiently, regardless of the collector bias voltage,  $\Delta V_c$ . In fact, for particles smaller than approximately 30 nm in diameter, the partial charging and lower ion attachment coefficients result in degraded collection efficiency with decreasing particle sizes (Zhuang et al. 2000; S.-H. Huang and Chen 2002; Adachi, Kousaka, and Okuyama 1985).

Figure 7 shows that, under the experimental conditions used in the present study, the prediction (Deutsch collection theory) based on Cochet's charging model is consistent with the experimentally measured trend of the fractional collection efficiency for particles larger than 100 nm. However, due in part to the limitation of Cochet's assumption of infinite particle charging time, the agreement is poor for particles smaller than 100 nm. For larger particles, where the field charging mechanism dominates, the assumption of infinite charging time is adequate as they readily reach saturation charge (Mizuno 2000; White 1951). However, for ultrafine particles where the diffusion charging is the dominant mechanism, longer relaxation time is necessary to gain sufficient charges (Adachi et al. 1985; Pui et al. 1988; White 1951).



The collection efficiency of the cylindrical configuration was similar to that of the rectangular configuration under comparable operating conditions. This implies that asymmetric electric fields in the rectangular collector have a small influence on the overall performance. However, the rectangular collector requires higher water-to-air mass flow rate ratios than the cylindrical collector. Cylindrical collector also requires less electrode area per unit footprint of the device. As such, cylindrical devices are more attractive for applications in large-scale applications for reduced electrode cost and exposed high-voltage surface area.

**Figure 7 here.**

Figure 7. Experimentally measured and predicted (Cochet's model) fractional collection efficiencies for the cylindrical and the rectangular WESP at different collector bias voltages. The experimental and predicted values are presented as the symbols and the lines, respectively.

Effects of air stream velocity

Figure 8 shows the experimentally measured and predicted (using equations 2-5) fractional collection efficiency for the cylindrical and the rectangular WESP as a function of the particle diameter for different air flow velocities. In these experiments, the water flow rate per string,  $\dot{m}_{Lps}$ , was fixed at 0.06 g/s. The air stream velocity in the collector was either set to 2.3 or 4.5 m/s, and the bias voltages for the particle pre-charger and the string collectors were 7.4 kV and 10 kV, respectively. The smaller air stream velocities result in larger fractional collection efficiencies for the entire range of particle diameters due to the longer residence times provided for both charging and collection processes. The comparison of the collection efficiencies obtained from the models (equations 2-5) with those of experiments in Figure 8 shows similar trends to those observed in Figure 7.

**Figure 8 here.**

Figure 8. Effect of the gas velocities in the collector on the experimentally measured and predicted (Cochet's model) fractional collection efficiencies for the cylindrical and the

rectangular WESP. The experimental results and predicted values are presented as the symbols and the lines, respectively.

### Numerical simulation results

We performed numerical simulation to help further examine particle collection in our string-based collectors. The average number of charges per particle,  $n_p$ , is not known *a priori*. This is further complicated by the fact that particles in the exhausts of a diesel generator are heterogeneous and their dielectric constants do not have a single constant value. Previous studies (Hinds 1999), for example, estimated the effective dielectric constant to be between 1 and 10. In view of this, we use an iterative approach to estimate the average number of charges per particle from our experimental data. That is, for particles of a given diameter, we adjust the corresponding  $n_p$  until the fractional collection efficiency obtained in our numerical simulation matches the experimental results (blue triangles in Figure 9(a)). We emphasize that our numerical simulation is intended to help interpret our experimental data rather than provide an independent validation of the data.

The fractional collection efficiency is calculated by dividing the number of particles that reach the surface of the string by the total number of particles released at the inlet. The prediction from Cochet's model agrees to within 15% with our results for particles larger than approximately 100 nm (Figure 9(a)). Cochet's model, however, overpredicts  $n_p$  for smaller particles. For the smallest particles, our results indicate partial charging ( $n_p < 1$ ), consistent with the earlier observation from Figure 7. The average numbers of charges obtained from the linear and cylindrical collectors are comparable, differing by less than 5%.

Figure 9(b) illustrates representative particle trajectories in the cylindrical collector under the bias voltage,  $\Delta V_c$ , of 10 kV. The air is set to travel upward at a velocity of 3 m/s, the diameter of particles is 0.1  $\mu\text{m}$ , the average number of elementary charges on each particle is 11.5, and the total number of particles released at the inlet is 100. The color bar indicates the magnitudes of particle velocities. The average speed of particles increases as particles travel downstream due to

the acceleration of particles in the radial direction caused by the electric field. The maximum particle velocity at the outlet is  $\sim 4.2$  m/s.

**Figure 9 here.**

Figure 9. (a) Number of charges on particles obtained using our numerical simulation and using Cochet's model as a function of the particle size. The numerical simulation and the Cochet's model results are presented as the symbols and the dashed line, respectively, and (b) Numerically simulated particle trajectories in the cylindrical collector (domain size =  $12.5 \text{ mm} \times 600 \text{ mm}$ , inlet airflow velocity =  $3 \text{ m/s}$ , number of particles at inlet =  $100$ , particle diameter,  $d_p = 0.1 \text{ }\mu\text{m}$ , average number of charges on the particle,  $Q_p = 11.5$ , applied voltage =  $10 \text{ kV}$ ).

We next performed a parametric study to help investigate the effects of the bead density and water flow rate on the collection efficiency. We varied the water flow rate from  $0.01$  to  $0.135 \text{ g/s}$  per string, which translates to bead spacing,  $S_b$ , in the range of  $20$  to  $360 \text{ mm}$ . Figure 10(a) shows the numerical simulation domain for the cylindrical collector with bead profiles along the string. The bead length,  $L_b$ , and the bead thickness,  $t_b$ , are set to  $4$  and  $1.5 \text{ mm}$ , respectively, based on the experimental observations.

Figure 10(b) shows the effect of the water flow rate per string on the experimentally obtained bead spacing,  $S_b$ , and the particle collection efficiency obtained from numerical simulation. In the numerical simulation, the particle diameter,  $d_p$  was  $0.1 \text{ }\mu\text{m}$  and the inlet airflow velocity was  $3 \text{ m/s}$ . The average number of charges on the particle,  $Q_p$ , was set to  $11.5$ , as in Figure 9(a). Figure 10(b) indicates that increasing the water flow rate per string significantly decreases the bead spacing, while the fractional collection efficiency remains approximately the same. This suggests that the deformation of electric field lines around the liquid beads has a small effect on particle collection. The experimental and numerical simulation results indicate that using our string-based counterflow collector, high particle collection efficiencies can be obtained with liquid-to-gas ratios as low as approximately  $0.0066 \text{ kg/kg}$ .

**Figure 10 here.**

Figure 10. (a) Schematics of the numerical simulation domain for the cylindrical WESP with bead profiles along the string. (b) Effect of the water flow rate per string on the bead spacing (obtained from experiments) and the collection efficiency (obtained from experiments and numerical simulation for particles with 0.1  $\mu\text{m}$  diameter). The experimental and numerical simulation results are presented as the solid and hollow symbols, respectively

## Conclusion

We experimentally and numerically studied a counter-flow WESP design that utilizes water films flowing down vertical strings. The strings are continuously supplied with water and act as collection plates for particles in the diameter range of 10 nm to 2.5  $\mu\text{m}$ . To quantify the performance of our string-based WESPs, the fractional collection efficiency was experimentally determined. We show that for water flow rates per string,  $\dot{m}_{\text{Lps}}$ , larger than 0.01 g/s, which corresponds to a water-to-air flow rate ratio of  $\sim 0.007$  kg/kg,  $\dot{m}_{\text{Lps}}$  has negligible effects on the collection efficiency of our particle collector. Consistent with other works on WESP, our experimental results also showed that increases in the collector bias voltage as well as the air residence time in the collector result in increased collection efficiencies. Furthermore, increase in collection efficiency due to increase in air residence time was more pronounced. The collection efficiency for particle sizes between 0.1 – 1  $\mu\text{m}$  increased by approximately 40% when air velocity is decreased by a factor of 2. In contrast, the same collection efficiency increased approximately 20% when string collector bias voltage is increased by a factor of 2.

We also show that, compared with previously reported WESP devices, our string-based design can achieve higher collection efficiencies with significantly lower water-to-air flow rate ratios. In addition, we also demonstrate that the present string-based counterflow WESP has competitive performance in capturing fine and ultrafine particles when compared with previous devices in terms of the particle collection efficiency and the air flow rate that can be handled per WESP volume. Our string based WESP offers a potential collection efficiency of up to 99% and has improved capability to treat larger volumes of air streams for a given device volume. Further

research is necessary to scale up and optimize the device designs for a wide variety of potential applications. In this connection, additional research efforts are also necessary to systematically investigate the effects of practical parameters, such as the air stream temperature and operation time, which were not examined in the present study.

### **Acknowledgment**

The authors would like to thank Samira Chizari for her contribution in the fabrication of the experimental setup.

### **Funding**

The present article is based on work supported by the US National Science Foundation through grant CBET-1358034 and the Simons Foundation Math+X investigator award number 510776.

Questions may be addressed to [abolfazlsad@ucla.edu](mailto:abolfazlsad@ucla.edu).

## References

- Adachi, M., Y. Kousaka, and K. Okuyama. 1985. "Unipolar and Bipolar Diffusion Charging of Ultrafine Aerosol Particles." *Journal of Aerosol Science* 16 (2): 109–23.  
doi:10.1016/0021-8502(85)90079-5.
- Adamiak, K. 2013. "Numerical Models in Simulating Wire-Plate Electrostatic Precipitators: A Review." *Journal of Electrostatics* 71 (4): 673–80. doi:10.1016/j.elstat.2013.03.001.
- Ali, M., H. Pasic, K. Alam, S. a. N. Tiji, N. Mannella, T. Silva, and T. Liu. 2016. "Experimental Study of Cross-Flow Wet Electrostatic Precipitator." *Journal of the Air & Waste Management Association (1995)* 66 (12): 1237–44.  
doi:10.1080/10962247.2016.1209258.
- Bai, Hsunling, Chungsyng Lu, and Chung Liang Chang. 1995. "A Model to Predict the System Performance of an Electrostatic Precipitator for Collecting Polydisperse Particles." *Journal of the Air & Waste Management Association* 45 (11): 908–16.  
doi:10.1080/10473289.1995.10467423.
- Bayless, David J., M. Khairul Alam, Roger Radcliff, and John Caine. 2004. "Membrane-Based Wet Electrostatic Precipitation." *Fuel Processing Technology, Air Quality III: Mercury, Trace Elements and Particulate Matter*, 85 (6): 781–98.  
doi:10.1016/j.fuproc.2003.11.025.
- Carotenuto, Claudia, Francesco Di Natale, and Amedeo Lancia. 2010. "Wet Electrostatic Scrubbers for the Abatement of Submicronic Particulate." *Chemical Engineering Journal* 165 (1): 35–45. doi:10.1016/j.cej.2010.08.049.
- Chen, Tzu-Ming, Chuen-Jinn Tsai, Shaw-Yi Yan, and Shou-Nan Li. 2014. "An Efficient Wet Electrostatic Precipitator for Removing Nanoparticles, Submicron and Micron-Sized Particles." *Separation and Purification Technology* 136 (November): 27–35.  
doi:10.1016/j.seppur.2014.08.032.
- Cochet, R. Lois. 1961. "Charge Des Fines Particules (Submicroniques) Etudes The'oretiques-Controles Re'cents Spectre de Particules." *Journal of Aerosol Science*, no. 102: 331–38.
- "COMSOL Multiphysics® Modeling Software." 2020. Accessed January 10.  
<https://www.comsol.com/>.

- Cooperman, P. 1971. "A New Theory of Precipitator Efficiency." *Atmospheric Environment* (1967) 5 (7): 541–51. doi:10.1016/0004-6981(71)90064-3.
- Deutsch, Walther. 1922. "Bewegung Und Ladung Der Elektrizitätsträger Im Zylinderkondensator." *Annalen Der Physik* 373 (12): 335–44. doi:10.1002/andp.19223731203.
- Dockery, D. W., C. A. Pope, X. Xu, J. D. Spengler, J. H. Ware, M. E. Fay, B. G. Ferris, and F. E. Speizer. 1993. "An Association between Air Pollution and Mortality in Six U.S. Cities." *The New England Journal of Medicine* 329 (24): 1753–59. doi:10.1056/NEJM199312093292401.
- Fiebig, Michael, Andreas Wiartalla, Bastian Holderbaum, and Sebastian Kiesow. 2014. "Particulate Emissions from Diesel Engines: Correlation between Engine Technology and Emissions." *Journal of Occupational Medicine and Toxicology (London, England)* 9 (March): 6. doi:10.1186/1745-6673-9-6.
- Flagan, Richard C., and John H. Seinfeld. 1988. *Fundamentals of Air Pollution Engineering*. Englewood Cliffs, New Jersey: Prentice-Hall, Inc. doi:https://authors.library.caltech.edu/25069/10/AirPollution88-Ch8.pdf.
- Haider, A., and O. Levenspiel. 1989. "Drag Coefficient and Terminal Velocity of Spherical and Nonspherical Particles." *Powder Technology* 58 (1): 63–70. doi:10.1016/0032-5910(89)80008-7.
- HEI. 2013. "Understanding the Health Effects of Ambient Ultrafine Particles." HEI Perspectives 3. Boston, MA: Health Effects Institute. <http://pubs.healtheffects.org/view.php?id=394>.
- Hesterberg, Thomas W., Christopher M. Long, William B. Bunn, Sonja N. Sax, Charles A. Lapin, and Peter A. Valberg. 2009. "Non-Cancer Health Effects of Diesel Exhaust: A Critical Assessment of Recent Human and Animal Toxicological Literature." *Critical Reviews in Toxicology* 39 (3): 195–227. doi:10.1080/10408440802220603.
- Hinds, William C. 1999. *Aerosol Technology: Properties, Behavior, and Measurement of Airborne Particles*. 2nd ed. New York: John Wiley & Sons, Inc.
- Huang, Chao, Xiuqin Ma, Meiyang Wang, Youshan Sun, Changping Zhang, and Huifen Tong. 2014. "Property of the PVC Dust Collecting Plate Used in Wet Membrane Electrostatic Precipitator." *IEEE Transactions on Plasma Science* 42 (11): 3520–28. doi:10.1109/TPS.2014.2359973.

- Huang, Sheng-Hsiu, and Chih-Chieh Chen. 2002. "Ultrafine Aerosol Penetration through Electrostatic Precipitators." *Environmental Science & Technology* 36 (21): 4625–32. doi:10.1021/es011157+.
- Jaworek, A., A. Marchewicz, A. T. Sobczyk, A. Krupa, and T. Czech. 2018. "Two-Stage Electrostatic Precipitators for the Reduction of PM<sub>2.5</sub> Particle Emission." *Progress in Energy and Combustion Science* 67 (July): 206–33. doi:10.1016/j.pecs.2018.03.003.
- Jewell-Larsen, Nels E., Sergey V. Karpov, Igor A. Krichtafovitch, Vivi Jayanty, Chih-Peng Hsu, and Alexander V. Mamishev. 2008. "Modeling of Corona-Induced Electrohydrodynamic Flow with COMSOL Multiphysics." In *Proceedings ESA Annual Meeting on Electrostatics, Minneapolis, Minnesota*, 17–19. Citeseer.
- Karanasiou, Angeliki, Mar Viana, Xavier Querol, Teresa Moreno, and Frank de Leeuw. 2014. "Assessment of Personal Exposure to Particulate Air Pollution during Commuting in European Cities—Recommendations and Policy Implications." *Science of The Total Environment* 490 (August): 785–97. doi:10.1016/j.scitotenv.2014.05.036.
- Kherbouche, F., Y. Benmimoun, A. Tilmatine, A. Zouaghi, and N. Zouzou. 2016. "Study of a New Electrostatic Precipitator with Asymmetrical Wire-to-Cylinder Configuration for Cement Particles Collection." *Journal of Electrostatics* 83 (October): 7–15. doi:10.1016/j.elstat.2016.07.001.
- Kim, Hak-Joon, Bangwoo Han, Yong-Jin Kim, Kyu-Dong Hwang, Won-Seek Oh, Seong-Yeon Yoo, and Tetsuji Oda. 2011. "Fine Particle Removal Performance of a Two-Stage Wet Electrostatic Precipitator Using a Nonmetallic Pre-Charger." *Journal of the Air & Waste Management Association (1995)* 61 (12): 1334–43. doi:10.1080/10473289.2011.603994.
- Kim, Hyeok-Gyu, Hong-Jik Kim, Myong-Hwa Lee, and Jong-Ho Kim. 2014. "Experimental Study on the Enhancement of Particle Removal Efficiency in Spray Tower Scrubber Using Electrospray." *Asian Journal of Atmospheric Environment* 8 (2): 89–95. doi:10.5572/ajae.2014.8.2.089.
- Kim, Ki-Hyun, Ehsanul Kabir, and Shamin Kabir. 2015. "A Review on the Human Health Impact of Airborne Particulate Matter." *Environment International* 74 (January): 136–43. doi:10.1016/j.envint.2014.10.005.
- Kim, Woojin, Heekyung An, Dongmok Lee, Woojong Lee, and Jae Hee Jung. 2015. "Development of a Novel Electrostatic Precipitator System Using a Wet-Porous



- Electrode Array.” *Aerosol Science and Technology* 49 (11). Taylor & Francis: 1100–1108. doi:10.1080/02786826.2015.1101051.
- Lane, Kevin J., Jonathan I. Levy, Madeleine K. Scammell, Junenette L. Peters, Allison P. Patton, Ellin Reisner, Lydia Lowe, Wig Zamore, John L. Durant, and Doug Brugge. 2016. “Association of Modeled Long-Term Personal Exposure to Ultrafine Particles with Inflammatory and Coagulation Biomarkers.” *Environment International* 92–93 (August): 173–82. doi:10.1016/j.envint.2016.03.013.
- Lawless, Phil A. 1996. “Particle Charging Bounds, Symmetry Relations, and an Analytic Charging Rate Model for the Continuum Regime.” *Journal of Aerosol Science* 27 (2): 191–215. doi:10.1016/0021-8502(95)00541-2.
- Lewtas, Joellen. 2007. “Air Pollution Combustion Emissions: Characterization of Causative Agents and Mechanisms Associated with Cancer, Reproductive, and Cardiovascular Effects.” *Mutation Research* 636 (1–3): 95–133. doi:10.1016/j.mrrev.2007.08.003.
- Li, Mingheng, and Panagiotis D. Christofides. 2006. “Collection Efficiency of Nanosize Particles in a Two-Stage Electrostatic Precipitator.” *Industrial & Engineering Chemistry Research* 45 (25): 8484–91. doi:10.1021/ie060101r.
- Liu, B. Y. H., and A. Kapadia. 1978. “Combined Field and Diffusion Charging of Aerosol Particles in the Continuum Regime.” *Journal of Aerosol Science* 9 (3): 227–42. doi:10.1016/0021-8502(78)90045-9.
- Liu, Benjamin Y. H., and Hsu-Chi Yeh. 1968. “On the Theory of Charging of Aerosol Particles in an Electric Field.” *Journal of Applied Physics* 39 (3): 1396–1402. doi:10.1063/1.1656368.
- Liu, Qi, Song-song Zhang, and Jian-pei Chen. 2015. “Numerical Analysis of Charged Particle Collection in Wire-Plate ESP.” *Journal of Electrostatics* 74 (April): 56–65. doi:10.1016/j.elstat.2014.11.007.
- Maricq, M. Matti. 2006. “On the Electrical Charge of Motor Vehicle Exhaust Particles.” *Journal of Aerosol Science* 37 (7): 858–74. doi:10.1016/j.jaerosci.2005.08.003.
- Miller, Bruce G. 2017. “8 - Particulate Formation and Control Technologies.” In *Clean Coal Engineering Technology (Second Edition)*, edited by Bruce G. Miller, 419–65. Butterworth-Heinemann. doi:10.1016/B978-0-12-811365-3.00008-9.

- Mizuno, A. 2000. "Electrostatic Precipitation." *IEEE Transactions on Dielectrics and Electrical Insulation* 7 (5): 615–24. doi:10.1109/94.879357.
- Morsi, S. A., and A. J. Alexander. 1972. "An Investigation of Particle Trajectories in Two-Phase Flow Systems." *Journal of Fluid Mechanics* 55 (2): 193–208. doi:10.1017/S0022112072001806.
- Ning, Z., C. S. Cheung, and S. X. Liu. 2004. "Experimental Investigation of the Effect of Exhaust Gas Cooling on Diesel Particulate." doi:10.1016/j.jaerosci.2003.10.001.
- Ohlwein, Simone, Ron Kappeler, Meltem Kutlar Joss, Nino Künzli, and Barbara Hoffmann. 2019. "Health Effects of Ultrafine Particles: A Systematic Literature Review Update of Epidemiological Evidence." *International Journal of Public Health* 64 (4): 547–59. doi:10.1007/s00038-019-01202-7.
- Pant, Pallavi, Gazala Habib, Julian D. Marshall, and Richard E. Peltier. 2017. "PM<sub>2.5</sub> Exposure in Highly Polluted Cities: A Case Study from New Delhi, India." *Environmental Research* 156 (July): 167–74. doi:10.1016/j.envres.2017.03.024.
- Park, Jeong-Ho, and Chung-Hwan Chun. 2002. "An Improved Modelling for Prediction of Grade Efficiency of Electrostatic Precipitators with Negative Corona." *Journal of Aerosol Science* 33 (4): 673–94. doi:10.1016/S0021-8502(01)00205-1.
- Parker, K. R., ed. 1997. *Applied Electrostatic Precipitation*. Springer Netherlands. doi:10.1007/978-94-009-1553-4.
- Pasic, H., J. Caine, and H. Shah. 2006. "MWESP: Membrane Tubular Wet Electrostatic Precipitators." *Filtration & Separation* 43 (9): 16–18. doi:10.1016/S0015-1882(06)71003-5.
- Pasic, Hajrudin, Md Khairul Alam, and David J. Bayless. 2001. Membrane electrostatic precipitator. United States US6231643B1, filed June 9, 1999, and issued May 15, 2001. <https://patents.google.com/patent/US6231643B1/en>.
- Pilat, Michael J. 1975. "Collection of Aerosol Particles by Electrostatic Droplet Spray Scrubbers." *Journal of the Air Pollution Control Association* 25 (2): 176–78. doi:10.1080/00022470.1975.10470070.
- Pope, C. Arden, Richard T. Burnett, Michael J. Thun, Eugenia E. Calle, Daniel Krewski, Kazuhiko Ito, and George D. Thurston. 2002. "Lung Cancer, Cardiopulmonary Mortality,

- and Long-Term Exposure to Fine Particulate Air Pollution.” *JAMA* 287 (9): 1132–41. doi:10.1001/jama.287.9.1132.
- Prasad, R., and Venkateswara R. Bella. 2011. “A Review on Diesel Soot Emission, Its Effect and Control.” *Bulletin of Chemical Reaction Engineering & Catalysis* 5 (2): 69–86. doi:10.9767/bcrec.5.2.794.69-86.
- Pui, David Y. H., Sheng-Chieh Chen, and Zhili Zuo. 2014. “PM<sub>2.5</sub> in China: Measurements, Sources, Visibility and Health Effects, and Mitigation.” *Particuology* 13 (April): 1–26. doi:10.1016/j.partic.2013.11.001.
- Riehle, C., and F. Löfer. 1995. “Grade Efficiency and Eddy Diffusivity Models.” *Journal of Electrostatics*, 5th International Conference on Electrostatic Precipitation, 34 (4): 401–13. doi:10.1016/0304-3886(94)00024-Q.
- Ristovski, Zoran D., Branka Miljevic, Nicholas C. Surawski, Lidia Morawska, Kwun M. Fong, Felicia Goh, and Ian A. Yang. 2012. “Respiratory Health Effects of Diesel Particulate Matter.” *Respirology (Carlton, Vic.)* 17 (2): 201–12. doi:10.1111/j.1440-1843.2011.02109.x.
- Sadeghpour, A., Z. Zeng, H. Ji, N. Dehdari Ebrahimi, A. L. Bertozzi, and Y. S. Ju. 2019. “Water Vapor Capturing Using an Array of Traveling Liquid Beads for Desalination and Water Treatment.” *Science Advances* 5 (4): eaav7662. doi:10.1126/sciadv.aav7662.
- Saiyisitpanich, Phirun, Tim C. Keener, Mingming Lu, Soon-Jai Khang, and Douglas E. Evans. 2006. “Collection of Ultrafine Diesel Particulate Matter (DPM) in Cylindrical Single-Stage Wet Electrostatic Precipitators.” *Environmental Science & Technology* 40 (24): 7890–95. doi:10.1021/es060887k.
- Su, Lipeng, Qian Du, Yide Wang, Heming Dong, Jianmin Gao, Min Wang, and Peng Dong. 2018. “Purification Characteristics of Fine Particulate Matter Treated by a Self-Flushing Wet Electrostatic Precipitator Equipped with a Flexible Electrode.” *Journal of the Air & Waste Management Association* 68 (7): 725–36. doi:10.1080/10962247.2018.1460635.
- Teng, Chenzi, Xing Fan, and Jian Li. 2020. “Effect of Charged Water Drop Atomization on Particle Removal Performance in Plate Type Wet Electrostatic Precipitator.” *Journal of Electrostatics* 104 (March): 103426. doi:10.1016/j.elstat.2020.103426.

- White, Harry J. 1951. "Particle Charging in Electrostatic Precipitation." *Transactions of the American Institute of Electrical Engineers* 70: 1186–91. doi:10.1109/T-AIEE.1951.5060545.
- Yang, Zhengda, Chenghang Zheng, Qianyun Chang, Yi Wan, Yi Wang, Xiang Gao, and Kefa Cen. 2017. "Fine Particle Migration and Collection in a Wet Electrostatic Precipitator." *Journal of the Air & Waste Management Association* 67 (4): 498–506. doi:10.1080/10962247.2016.1260074.
- Yoo, Kyung Hoon, Joon Sik Lee, and Myung Do Oh. 1997. "Charging and Collection of Submicron Particles in Two-Stage Parallel-Plate Electrostatic Precipitators." *Aerosol Science and Technology* 27 (3): 308–23. doi:10.1080/02786829708965476.
- Zeng, Zezhi, Abolfazl Sadeghpour, and Y. Sungtaek Ju. 2019. "A Highly Effective Multi-String Humidifier with a Low Gas Stream Pressure Drop for Desalination." *Desalination* 449 (January): 92–100. doi:10.1016/j.desal.2018.10.017.
- Zhibin, Zhao, and Zhang Guoquan. 1994. "Investigations of the Collection Efficiency of an Electrostatic Precipitator with Turbulent Effects." *Aerosol Science and Technology* 20 (2): 169–76. doi:10.1080/02786829408959674.
- Zhuang, Ye, Yong Jin Kim, Tai Gyu Lee, and Pratim Biswas. 2000. "Experimental and Theoretical Studies of Ultra-Fine Particle Behavior in Electrostatic Precipitators." *Journal of Electrostatics* 48 (3): 245–60. doi:10.1016/S0304-3886(99)00072-8.
- Zukeran, A., Y. Ikeda, Y. Ehara, M. Matsuyama, T. Ito, T. Takahashi, H. Kawakami, and T. Takamatsu. 1999. "Two-Stage-Type Electrostatic Precipitator Re-Entrainment Phenomena under Diesel Flue Gases." *IEEE Transactions on Industry Applications* 35 (2): 346–51. doi:10.1109/28.753627.

## List of Figure Captions:

- Figure 1. Schematic of the experimental setup for characterizing the performance of the string-based collectors. .... 6
- Figure 2. Schematics of (a) the rectangular and (b) the cylindrical configuration on the left and (c) the particle pre-charger and the front view of the particle pre-charger used in this study on the right. .... 7
- Figure 3. Schematics of the numerical simulation domains for (a) the rectangular WESP and (b) the cylindrical WESP. .... 9
- Figure 4. (a) Voltage-current curve and (b) average particle size distribution at the inlet of the particle pre-charger. .... 12
- Figure 5. Effect of the water flow rate per string on the fractional collection efficiency of the cylindrical WESP. .... 12
- Figure 6. Collection efficiencies as a function of the liquid-to-gas flow rate ratio for different WESP devices. We compare our device with previously reported WESP devices; electrostatic droplet spray (Pilat 1975), cylindrical WESP for DPM (Saiyasitpanich et al. 2006), flat-plate WESP (H.-J. Kim et al. 2011), electro spray tower scrubber (H.-G. Kim et al. 2014), cross flow string-based WESP (Ali et al. 2016), wire-to-plate WESP (Yang et al. 2017), and self-flushing WESP (Su et al. 2018). .... 13
- Figure 7. Experimentally measured and predicted (Cochet's model) fractional collection efficiencies for the cylindrical and the rectangular WESP at different collector bias voltages. The experimental and predicted values are presented as the symbols and the lines, respectively. .... 15
- Figure 8. Effect of the gas velocities in the collector on the experimentally measured and predicted (Cochet's model) fractional collection efficiencies for the cylindrical and the rectangular WESP. The experimental results and predicted values are presented as the symbols and the lines, respectively. .... 15
- Figure 9. (a) Number of charges on particles obtained using our numerical simulation and using Cochet's model as a function of the particle size. The numerical simulation and the Cochet's model results are presented as the symbols and the dashed line, respectively, and (b) Numerically simulated particle trajectories in the cylindrical collector (domain size =

12.5 mm × 600 mm, inlet airflow velocity = 3 m/s, number of particles at inlet = 100, particle diameter,  $d_p = 0.1 \mu\text{m}$ , average number of charges on the particle,  $Q_p = 11.5$ , applied voltage = 10 kV). ..... 17

Figure 10. (a) Schematics of the numerical simulation domain for the cylindrical WESP with bead profiles along the string. (b) Effect of the water flow rate per string on the bead spacing (obtained from experiments) and the collection efficiency (obtained from experiments and numerical simulation for particles with  $0.1 \mu\text{m}$  diameter). The experimental and numerical simulation results are presented as the solid and hollow symbols, respectively ..... 18

ACCEPTED MANUSCRIPT

### **About the Author**

Abolfazl Sadeghpour, Ph.D., graduated from the University of California Los Angeles with a research focus on designing novel mass and heat exchangers. E-mail: abolfazlsad@ucla.edu.

Contact information: Mechanical and Aerospace Engineering Department, University of California, Los Angeles, 420 Westwood Plaza, Los Angeles, California 90095, United States.

Farzan Oroumiyeh is a Ph.D. candidate at the University of California, Los Angeles, performing research on PM emission of cars due to breaks.

Danny D. Ko is a Ph.D. student at the University of California, Los Angeles.

Yifang Zhu is a professor at the University of California, Los Angeles.

H. Ji is a post-doc scholar at the University of California, Los Angeles.

A. L. Bertozzi is a professor at the University of California, Los Angeles.

Y. Sungtaek Ju is a professor at the University of California, Los Angeles.

ACCEPTED MANUSCRIPT

Table 3. Parameters and test conditions used to study the string-based WESP performance.

Parameters	Conditions	Notes
Applied voltage [kV]	0 - 10	Bias voltage for string collectors, $\Delta V_c$
	7 - 7.6	Bias voltage for particle pre-charger, $\Delta V_p$
Air velocity [m/s]	2.3 – 4.5	In WESP
	0.7 - 1.5	In particle pre-charger
Water flow rate per string [g/s]	0.01 – 0.135	$\dot{m}_{Lps}$
Air inlet temperature [°C]	30 - 40	---



Table 4. Comparison of the experimental conditions and performance metrics of the present design with those of previous WESP designs.

Collection type	Particle diameter [μm]	Water flow rate [kg/s]	Air flow rate [kg/s]	Air velocity [m/s]	Collection efficiency [%]	Air flow rate /collector volume [(m <sup>3</sup> /s) /m <sup>3</sup> ]	Liquid to gas flow ratio [kg/s / kg/s]
Cylindrical WESP (Saiyasitpanich et al. 2006)	0.02-0.8	0.05	0.056	2.3	90 – 99	2.5	0.89
Single-stage parallel plate WESP (Lin et al. 2010)	0.02-0.6	0.0005	0.0008	0.076	97 – 99.7	0.538	6.25
Flat-plate WESP (H.-J. Kim et al. 2011)	0.02-0.5	0.003	0.0016	1	70 – 95	2.4	1.88
PVC cylindrical WESP (J. -H. Kim et al. 2012)	0.05 – 2	0.0083	0.0035	1	99 – 99.7	2.44	2.37
Cross flow string based WESP (Ali et al. 2016)	1.61-8.84	0.04	3.24	3	60 – 80	1.25	0.012
Membrane based WESP (Wang et al. 2016)	0.01-10	10 <sup>-4</sup>	0.002	0.4	65 – 93	2.67	0.05
Spray-type WESP (Du et al. 2016)	0.3-2.5	0.0042	0.181	2.35	35 – 69	0.783	0.023
Wire-to-plate WESP (Yang et al. 2017)	0.02-9	0.03	0.03	1.16	85 – 99	1.1	1
Pulsed corona WESP (Kuroki et al. 2017)	0.02 – 0.4	0.0004	7 x 10 <sup>-5</sup>	0.21	80 – 99	0.816	6.246
Self-flushing WESP (Su et al. 2018)	0.07-2.5	0.007	0.031	3	60 – 72	1	0.22
Charged water drop WESP	0.02-3.8	0.001	0.013	0.19	93 – 99	0.78	0.077

(Teng et al. 2020)

String-based Cylindrical WESP (Present study)	0.01-2.5	$10^{-5}$	0.0015	3	80 – 99	4.36	0.0066
---	----------	-----------	--------	---	---------	------	--------

---

---

Wet Electrostatic Precipitators (WESPs) are highly effective for collecting fine particles in exhaust air streams from various sources such as diesel engines, power plants, and oil refineries. However, their large-scale adoption has been limited by high water usage and reduced collection efficiencies for ultrafine particles. We perform experimental and numerical investigation to characterize the collection efficiency and water flow rate-dependence of a new design of WESP. The string-based counterflow WESP reported in this study offers number-based collection efficiencies  $> 70\%$  at air flow rates per collector volume as high as  $4.36 \text{ (m}^3/\text{s)/m}^3$  for particles of diameters ranging from  $10 \text{ nm} - 2.5 \text{ }\mu\text{m}$ , while significantly reducing water usage. Our work provides a basis for the design of more compact and water-efficient WESPs.

Implications Statement

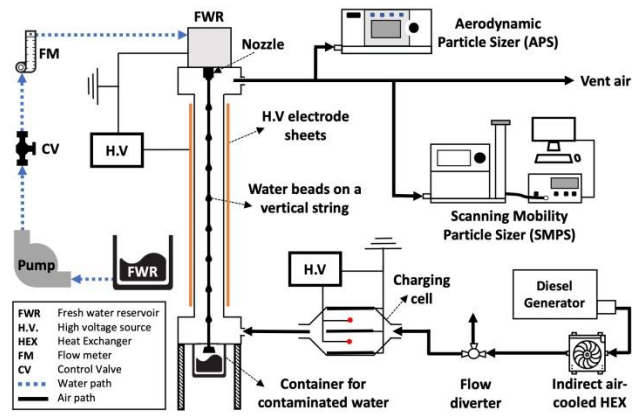


Fig 1

ACCEPTED MANUSCRIPT

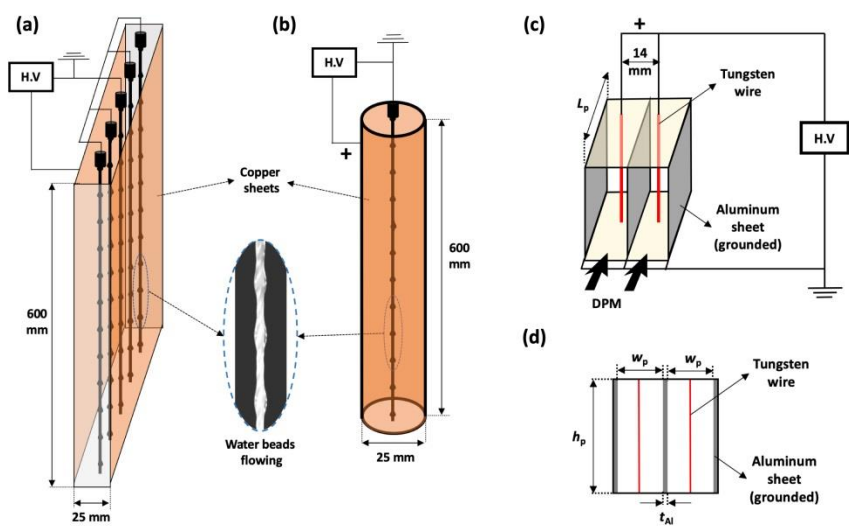


Fig 2

ACCEPTED MAN

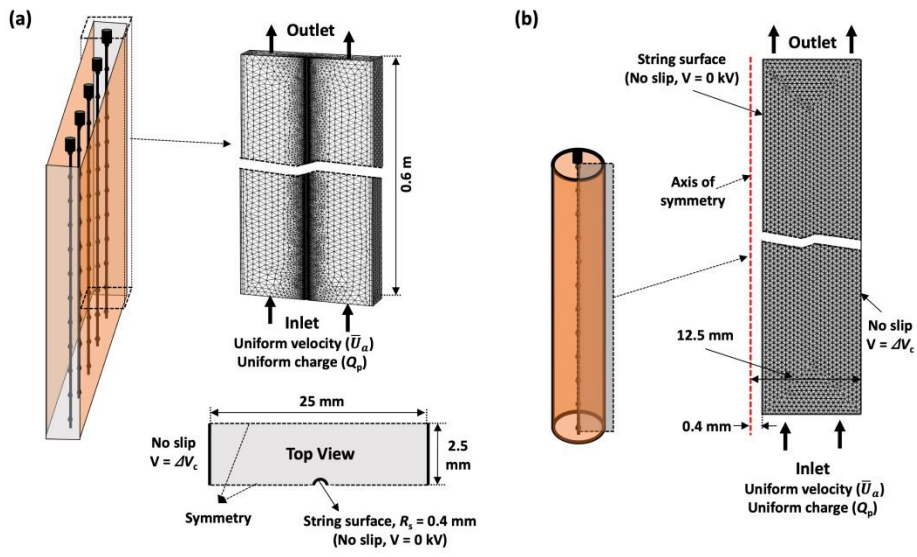


Fig 3

ACCEPTED MAN

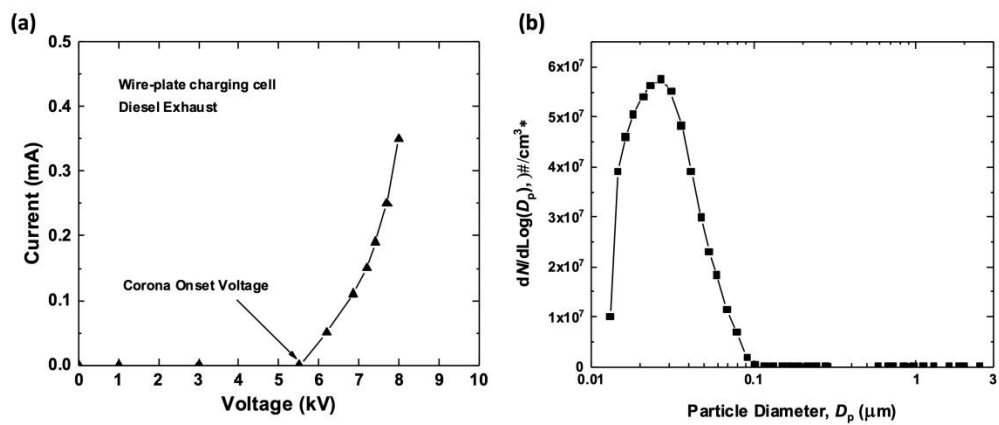


Fig 4

ACCEPTED MAN

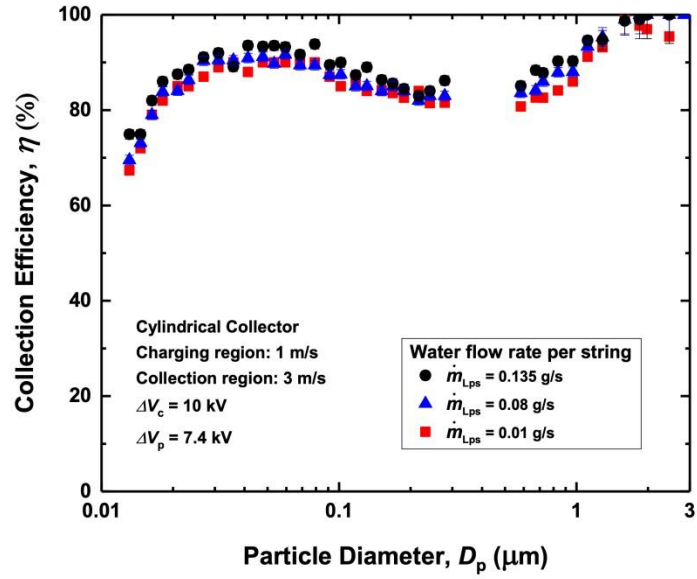


Fig 5

ACCEPTED MAN

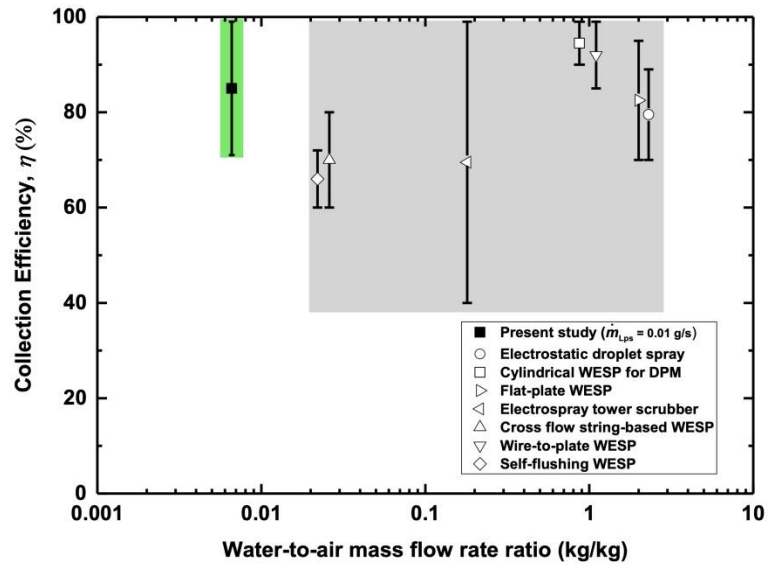


Fig 6

ACCEPTED MANUSCRIPT



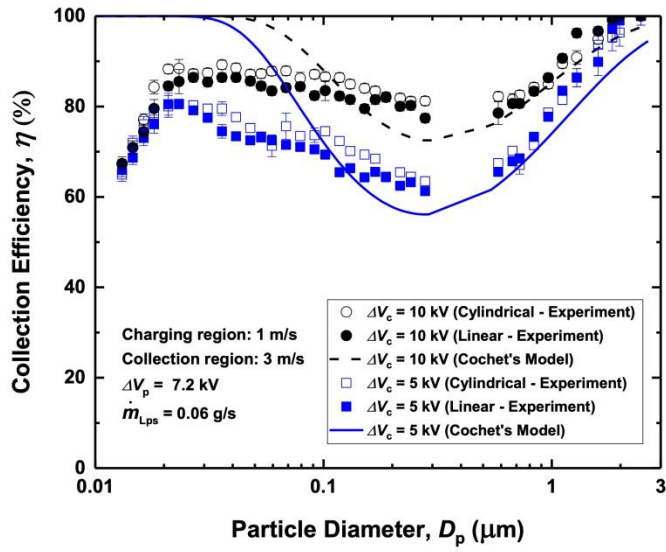


Fig 7

ACCEPTED MAN

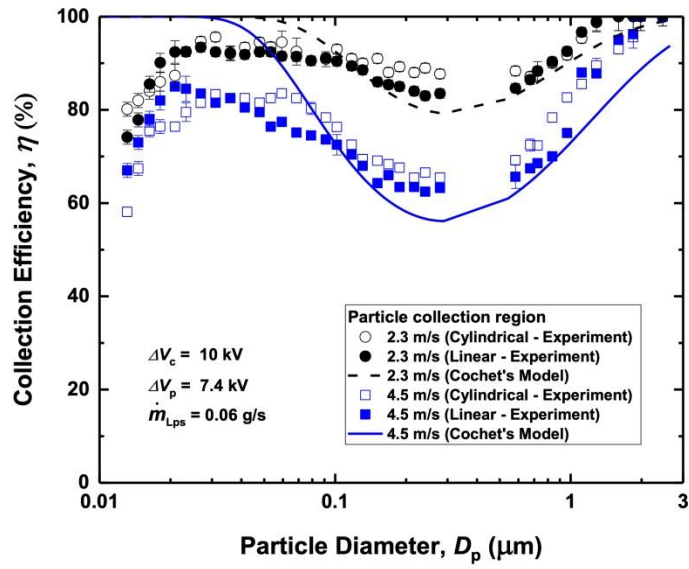


Fig 8

ACCEPTED MAN

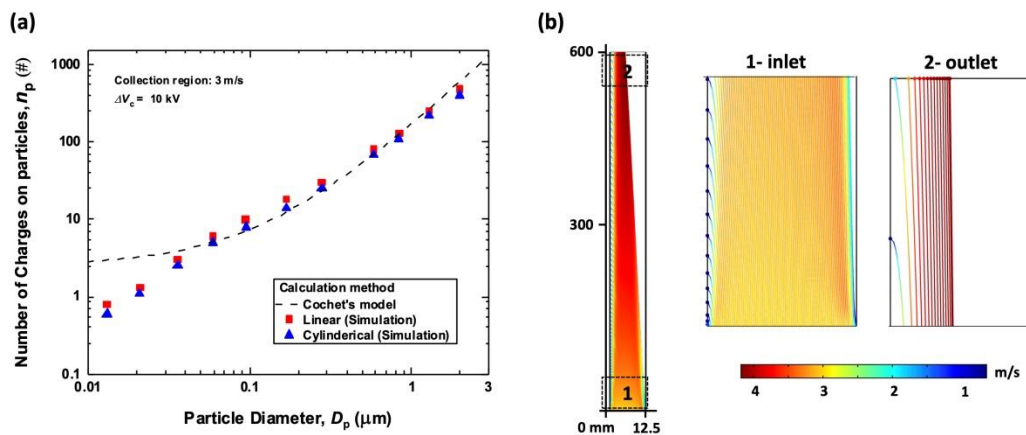


Fig 9

ACCEPTED MANUSCRIPT

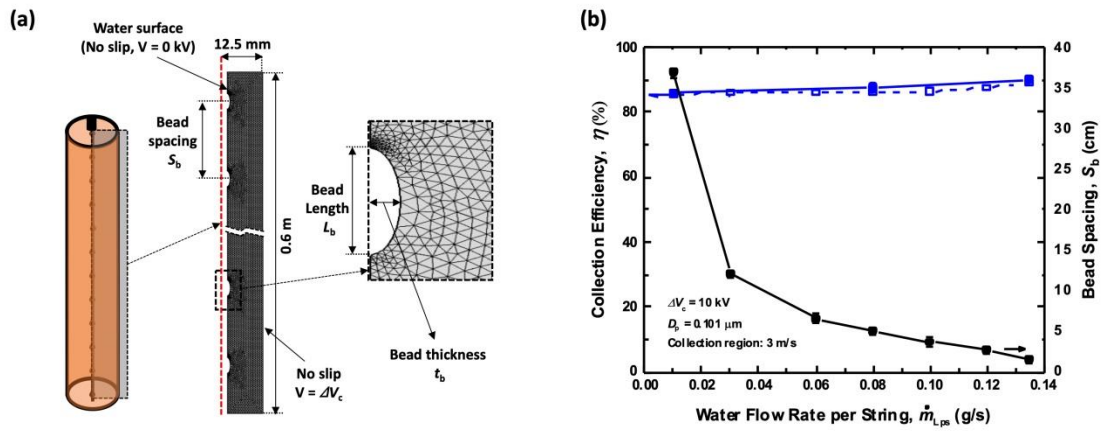


Fig 10

ACCEPTED MAN